Volume 15
Number 12
December 2024
Pages 3915–4226

RSC Medicinal Chemistry

rsc.li/medchem

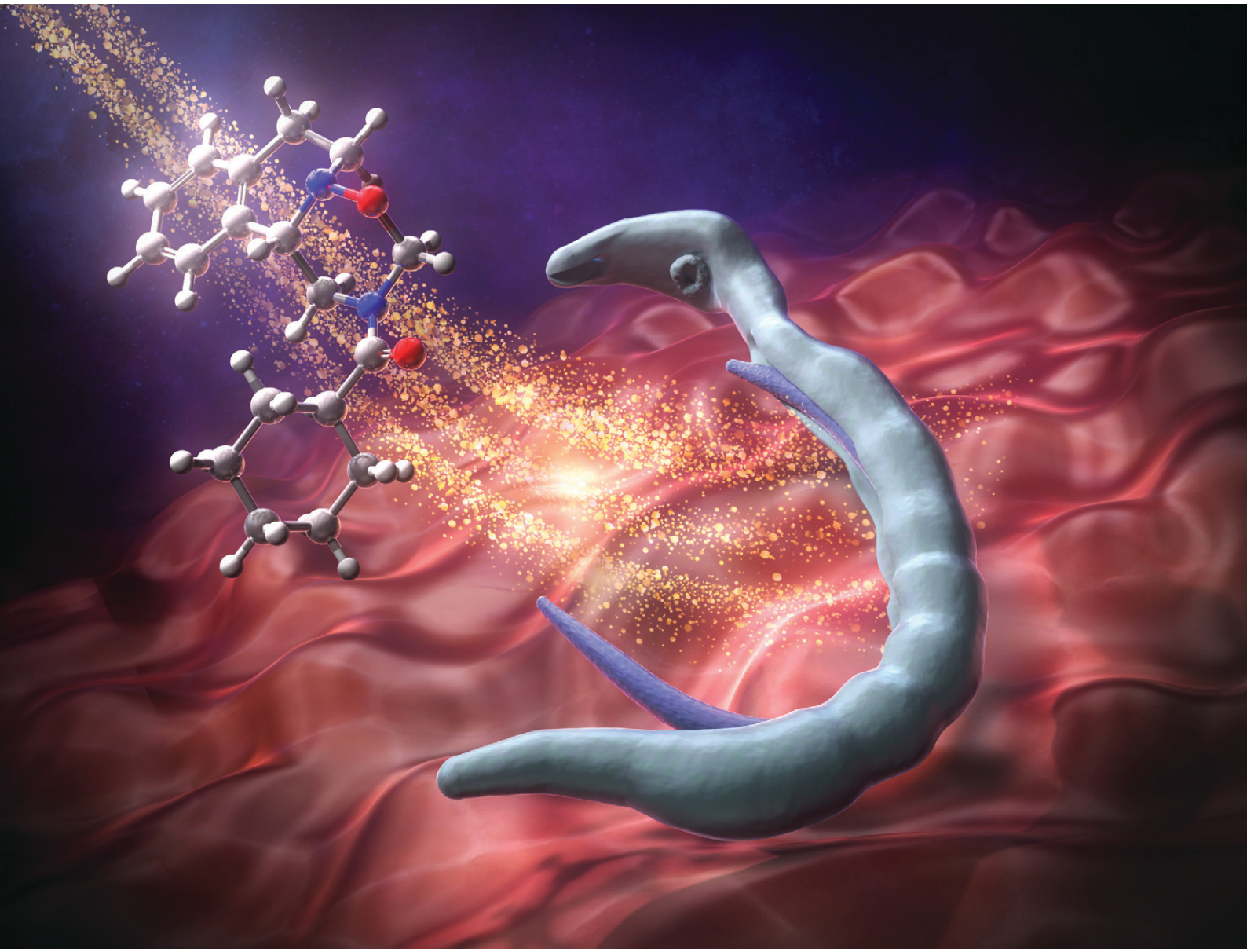

ISSN 2632-8682

ROYAL SOCIETY OF CHEMISTRY

RESEARCH ARTICLE

Kennosuke Itoh *et al.*

Anti-Schistosomal activity and ADMET properties of 1,2,5-oxadiazinane-containing compound synthesized by visible-light photoredox catalysis

RSC Medicinal Chemistry

ROYAL SOCIETY OF CHEMISTRY

RESEARCH ARTICLE

View Article Online
View Journal | View Issue

Cite this: *RSC Med. Chem.*, 2024, **15**, 4001

Anti-Schistosomal activity and ADMET properties of 1,2,5-oxadiazinane-containing compound synthesized by visible-light photoredox catalysis†

Kennosuke Itoh, *[ab] Hiroki Nakahara, [a] Atsushi Takashino,[a] Aya Hara,[a] Akiho Katsuno,[a] Yuriko Abe,[a] Takaaki Mizuguchi, [ab] Fumika Karaki, [ab] Shigeto Hirayama,[ab] Kenichiro Nagai, [b] Reiko Seki,[b] Noriko Sato,[b] Kazuki Okuyama,[c] Masashi Hashimoto,[c] Ken Tokunaga, [d] Hitoshi Ishida, [e] Fusako Mikami,[f] Kofi Dadzie Kwofie,[f] Hayato Kawada,[f] Bangzhong Lin,[g] Kazuto Nunomura,[g] Toshio Kanai,[g] Takeshi Hatta,[f] Naotoshi Tsuji,[f] Junichi Haruta[g] and Hideaki Fujii [ab]

The incorporation of saturated nitrogen-containing heterocycle 1,2,5-oxadiazinane into small molecules represents a compelling avenue in drug discovery due to its unexplored behavior within biological systems and incomplete protocols for synthesis. In this study, we present 1,2,5-oxadiazinane, an innovative heterocyclic bioisostere of piperizin-2-one and novel chemotype of the *anti*-schistosomal drug praziquantel (PZQ), which has been the only clinical drug available for three decades. PZQ is associated with significant drawbacks, including poor solubility, a bitter taste, and low metabolic stability. Therefore, the discovery of a new class of *anti*-schistosomal agents is imperative. To address this challenge, we introduce a pioneering method for the synthesis of 1,2,5-oxadiazinane derivatives through the cycloaddition of nitrones with *N*,*N*,*N*′,*N*′-tetraalkyldiaminomethane in the presence of an Ir^{III} complex photosensitizer. This transformative reaction offers a streamlined route to various kinds of 1,2,5-oxadiazinanes that is characterized by mild reaction conditions and broad substrate scope. Mechanistic investigations suggest that the photoredox pathway underlies the [3 + 3] photocycloaddition process. Thus, based on bioisosteric replacement, we identified a remarkable molecule as a new chemotype of a potent *anti*-schistosomal compound that not only exhibits superior solubility, but also retains the potent biological activity inherent to PZQ.

Received 3rd August 2024,
Accepted 14th September 2024

DOI: 10.1039/d4md00599f

rsc.li/medchem

Introduction

As vital scaffolds for designing and developing novel drugs, saturated nitrogen-containing heterocycles have immense potential for the field of drug development.[1] Their sp^3 hybridized atoms, providing three-dimensional shapes in drug candidates and facilitating multiple interactions with biological systems, are key to the effectiveness of these molecules.[2,3] Moreover, they can significantly improve the pharmacokinetic/pharmacodynamic (PK/PD) properties of drug candidates, thereby increasing their clinical success rates.[4] Given these promising attributes, the proposition of novel synthetic methodologies for saturated nitrogen-containing heterocycles is not just fascinating, but a compelling avenue of investigation.[5–12]

Our research has been focused on the prospect of integrating a saturated nitrogen-containing heterocycle, 1,2,5-oxadiazinane, instead of the incumbent moiety piperazin-2-one, which is present in FDA-approved drugs. Notable examples include the *anti*-schistosomal agent praziquantel (PZQ),[13–15] along with the antiretroviral drugs dolutegravir,

[a] *Laboratory of Medicinal Chemistry, School of Pharmacy, Kitasato University, 5-9-1 Shirokane, Minato-ku, Tokyo 108-8641, Japan.*
E-mail: itok@pharm.kitasato-u.ac.jp
[b] *Medicinal Research Laboratories, School of Pharmacy, Kitasato University, 5-9-1 Shirokane, Minato-ku, Tokyo 108-8641, Japan*
[c] *Department of Material Science, Graduate School of Science, Josai University, 1-1 Keyakidai, Sakado, Saitama 350-0295, Japan*
[d] *Division of Liberal Arts, Center for Promotion of Higher Education, Kogakuin University, 2665-1 Nakano-machi, Hachioji, Tokyo 192-0015, Japan*
[e] *Graduate School of Science and Engineering, Department of Chemistry, Materials and Bioengineering, Kansai University, 3-3-35 Yamate-cho, Suita, Osaka, 564-8680, Japan*
[f] *Department of Parasitology and Tropical Medicine, Kitasato University School of Medicine, 1-15-1 Kitazato, Minami-ku, Sagamihara, Kanagawa 252-0374, Japan*
[g] *Drug Innovation Center Lead Exploration Unit, Graduate School of Pharmaceutical Sciences, Osaka University, 1-6 Yamadagaoka, Suita, Osaka 565-0871, Japan*

† Electronic supplementary information (ESI) available: The data that support the findings of this study are available in the ESI of this article. Videos for the worm movement assay are also included. CCDC 2224678. For ESI and crystallographic data in CIF or other electronic format see DOI: **https://doi.org/10.1039/d4md00599f**

bictegravir, and cabotegravir,[16] which are renowned for their efficacy against human immunodeficiency virus (HIV) (Scheme 1a). This approach, which can be advocated as a bioisosteric replacement strategy, revolutionizes drug design by ingeniously replacing an atom or functional group with another. This method not only improves the physicochemical and ADMET (absorption, distribution, metabolism, excretion, and toxicity) properties of molecules, but maintains their biological efficacy.[17,18] The pharmaceutical agents referenced above belong to biopharmaceutics classification system (BCS) class II, which is characterized by high permeability and low solubility.[19] Consequently, their gastrointestinal dissociation rates are sluggish, leading to limited bioavailability. In such instances, bioisosteric replacement has proven effective in enhancing the intrinsic properties of these drugs.

Of particular interest is PZQ, which has been exclusively employed as a therapeutic agent for schistosomiasis—one of the neglected tropical diseases—for over three decades, with no other agent surpassing it to this day.[20] However, despite its long-standing clinical use, PZQ is plagued by unresolved issues, including low solubility,[21,22] poor metabolic stability,[23] and a bitter taste.[24] In 2012, the Global Health Innovative Technology Fund (GHIT), along with Merck & Co., Inc., the Bill and Melinda Gates Foundation, and the European & Developing Countries Clinical Trials Partnership (EDCTP), established the Pediatric Praziquantel Consortium to address this challenge.[25] Through their dedicated efforts, they successfully developed arPraziquantel (L-praziquantel), a chiral switch for PZQ, as well as orodispersible tablets. In 2023, they received a positive scientific opinion on arPraziquantel from the European Medicines Agency (EMA).[26,27] Very recently, in 2024, Sprague, Marchant, and colleagues merely discovered a new chemotype of *anti*-schistosomal agent.[28] Regarding the low solubility of PZQ in aqueous media, the carbonyl group of the piperazin-2-one ring does not appear to increase the solubility of PZQ, as the molecule contains rings that lack polarity or are weakly polarized. However, crystallographic analyses indicate that the carbonyl oxygen of piperazin-2-one plays a pivotal role in mediating intermolecular hydrogen bonding, thereby contributing to the overall aggregation and reduced solubility.[29] Although replacing the piperazine ring with the piperazin-2-one ring of PZQ presents a viable strategy for disrupting these hydrogen-bonding interactions, it unfortunately results in a complete loss of biological activity in the resulting piperazine derivative.[20b,30] This underscores the critical importance of the carbonyl oxygen within the piperazin-2-one ring of PZQ for exerting its *anti*-schistosomal effects. Consequently, the prospect of bioisosteric replacement within PZQ by substituting the piperazin-2-one ring with a 1,2,5-oxadiazinane ring presents a significant challenge. However, it remains feasible due to the non-classical isosteric relationship between divalent ether oxygen and the carbonyl group.[31] The embedded oxygen atom can compensate for the role of the carbonyl oxygen, maintaining essential interactions with the Schistosoma target molecule while ameliorating the solubility provided by the weakened intermolecular hydrogen bonding attributed to the carbonyl oxygen of the piperazin-2-one ring in PZQ.

In this study, we present a pioneering approach to bioisosteric replacement wherein the piperazin-2-one ring is replaced with the 1,2,5-oxadiazinane ring to yield a new chemotype of potent *anti*-schistosomal molecule, an unprecedented achievement (Scheme 1b). To build a 1,2,5-oxadiazinane ring, we developed efficient cycloaddition reactions between a diverse array of nitrones and *N*,*N*,*N*′,*N*′-tetraalkyldiaminomethanes in the presence of iridium(III) complex photosensitizer (Ir^{III} complex) (Scheme 1c). This methodology facilitated the synthesis of a wide range of 1,2,5-oxadiazinane derivatives. In contrast, thermal reactions[32] and an ultraviolet-induced process[33] are challenging. Furthermore, we elucidated the plausible mechanism underlying the photocycloaddition reaction and demonstrated the scalability of our approach by performing gram-scale synthesis of a 1,2,5-oxadiazinane derivative utilizing a custom-designed photochemical flow reactor. The present integrated study not only expands the chemical diversity accessible through bioisosteric replacement, but offers practical insights into the synthesis and mechanistic understanding of 1,2,5-oxadiazinane derivatives.

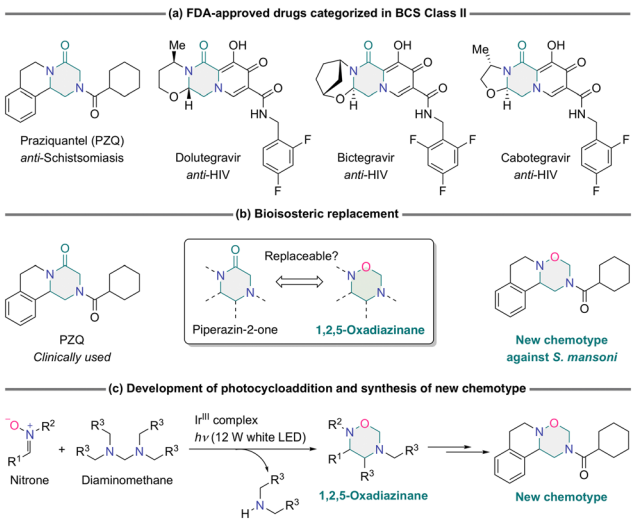

Scheme 1 Overview of the context of the research.

Results and discussion

Reaction optimization

Initially, we screened Ir^{III} complexes **I–XI** to evaluate their abilities to promote the cycloaddition reactions of nitrone **1a** (50 mM) with *N*,*N*,*N*′,*N*′-tetramethyldiaminomethane (**2a**) (500 mM) under high-intensity light irradiation (12 W white LEDs), leading to the formation of 1,2,5-oxadiazinane **3aa** (Table 1). Notably, in the absence of an Ir^{III} complex, no reaction was observed, and **1a** was recovered (entry 1). Ir^{III} complexes **I** and **II** yielded only trace amounts of **3aa** (entries 2 and 3), whereas Ir^{III} complexes **III**, **IV**, **V**, and **VI** exhibited limited promotion of the cycloaddition reactions, resulting in low yields of **3aa** (entries 4–7) and the formation of dimethylamine as a byproduct. Ir^{III} complex **VII** facilitated the desired reaction to afford a moderate yield of **3aa**

Table 1 Screening of photosensitizers[a]

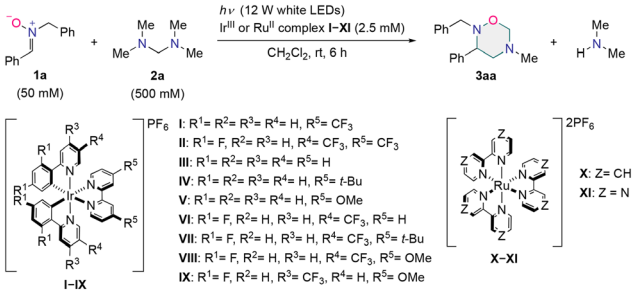

Entry	[M][b]	Yield[c] (%)	E^{*}[d] ($M^{n}*/M^{n-1}$)	$E_{1/2}$[d] (M^{n}/M^{n-1})
1[c]	None	0	None	None
2	**I**	Trace	+1.22	−0.88
3	**II**	Trace	+1.65	−0.79
4	**III**	21	+0.81	−1.31
5	**IV**	19	+0.66	−1.51
6	**V**	17	+1.03	−1.44
7	**VI**	46	+0.97	−1.23
8	**VII**	67	+1.21	−1.37
9	**VIII**	86	+1.41	−1.26
10[e]	**VIII**	82	+1.41	−1.26
11[f]	**VIII**	46	+1.41	−1.26
12	**IX**	65	+1.37	−1.26
13[g]	**X**	0	+0.77	−1.33
14[g]	**XI**	0	+1.45	−0.80

[a] Experiments were conducted using nitrone **1a** and *N*,*N*,*N*′,*N*′-tetramethyldiaminomethane (**2a**) in deaerated CH_2Cl_2 employing an Ir^{III} complex and irradiated with a 1-m LED strip (λ = 400–780 nm, 12 W, 60 white LEDs per m). [b] M = Ir or Ru. [c] Isolated yield. [d] Electrical potentials are provided in ref. 34, 35, and the ESI,† with units in volts. [e] 0.5 mM of **VIII** was used, and the reaction time was 94 h. [f] 100 mM of **2a** was used. [g] The reaction time was 24 h.

(entry 8), whereas Ir^{III} complex **VIII** emerged as the optimal mediator, resulting in a good yield of **3aa** (entry 9). Reducing the amount of **VIII** slowed the reaction, which was complete in 94 hours, yielding **3aa** in a comparable yield to entry 9 (entry 10). Decreasing the concentration of **2a** (100 mM) led to a decrease in the yield of **3aa** (entry 11). Compared with **VIII**, which features a CF_3 group at position 5, the newly prepared Ir^{III} complex **IX**, with a CF_3 group at position 4 of the pyridine ring in the ppy ligand, decelerates the desired reaction, resulting in a lower yield of **3aa** (entry 12). Conversely, ruthenium(II) (Ru^{II}) complexes **X** and **XI** were not suitable as photochemical mediators (entries 13 and 14). Considering the redox potential of the excited states [E^{*} ($Ir^{III}*/Ir^{II}$) and E^{*} ($Ru^{II}*/Ru^{I}$)] and ground states [$E_{1/2}$ (Ir^{III}/Ir^{II}) and $E_{1/2}$ (Ru^{II}/Ru^{I})] of the Ir^{III} complexes and Ru^{II} complexes,[34,35] the ideal complex should function as a potent oxidizing reagent for **2a** and a powerful one-electron-reducing reagent for the reaction intermediate. Ultimately, Ir^{III} complex **VIII** emerged as the optimal photosensitizer, distinguished by its remarkable oxidizing ability [E^{*} ($Ir^{III}*/Ir^{II}$) = +1.41 V] and one-electron-reducing ability [$E_{1/2}$ (Ir^{III}/Ir^{II}) = −1.26 V] (Fig. S3, Tables S2 and S3†). The presence of fluorine groups in the ppy ligands of Ir^{III} complexes **VI**–**IX** likely reduces the phosphorescence radiative rate constant and spin-orbit coupling strength of the photoexcited species.[36] The above-mentioned photophysical phenomena would lead to an increased triplet lifetime of the Ir^{III} complexes, ultimately improve the reaction efficiency. Additionally, the screening results suggest that Ir^{III} complexes play a crucial role in facilitating a reductive quenching process that promotes photocycloaddition.[37] Furthermore, **1a** was recovered in the absence of **2a**, indicating the absence of photodecomposition and the stability of **1a** in the presence of the photoexcited Ir^{III} complex. This accentuates the indispensable role of **2a** in inducing the desired reaction. Employing CH_2Cl_2 as the solvent yielded the best results compared to other solvents (MeCN: 8 h, 65% yield; MeOH: 25 h, 29%).

Scope

Having established the optimized reaction conditions, our investigation focused on exploring the scope of nitrones **1b**–**1u** and *N*,*N*,*N*′,*N*′-tetraalkyldiaminomethanes **2b**–**2d** (Scheme 2). Reactions involving **1b**–**1l**, featuring aryl, heteroaryl, and cyclohexyl groups as R^1, and **2a** gave **3ba**–**3la**, with low to moderate yield. Notably, *N*-*tert*-butyl nitrone **1m** and π-extended derivatives **1n**–**1s**, which are susceptible to decomposition under UV irradiation,[33] underwent successful cyclization to afford **3ma**–**3sa** in this visible-light-driven reaction. Reactions employing cyclic nitrones **1t** and **1u** proceeded smoothly, yielding tricyclic **3ta** and tetracyclic **3ua** products. *N*,*N*,*N*′,*N*′-tetraalkyldiaminomethanes **2b**–**2e** in reactions with **1a**, **1t**, and **1u** yielded **3ab**, **3tb**, **3ub**, **3uc**, **3ud**, and **3ue** in low to reasonable yields. We successfully conducted single-crystal X-ray diffraction analysis of **3ab** and determined the relative stereochemistry of **3ue** as *trans* in NMR.

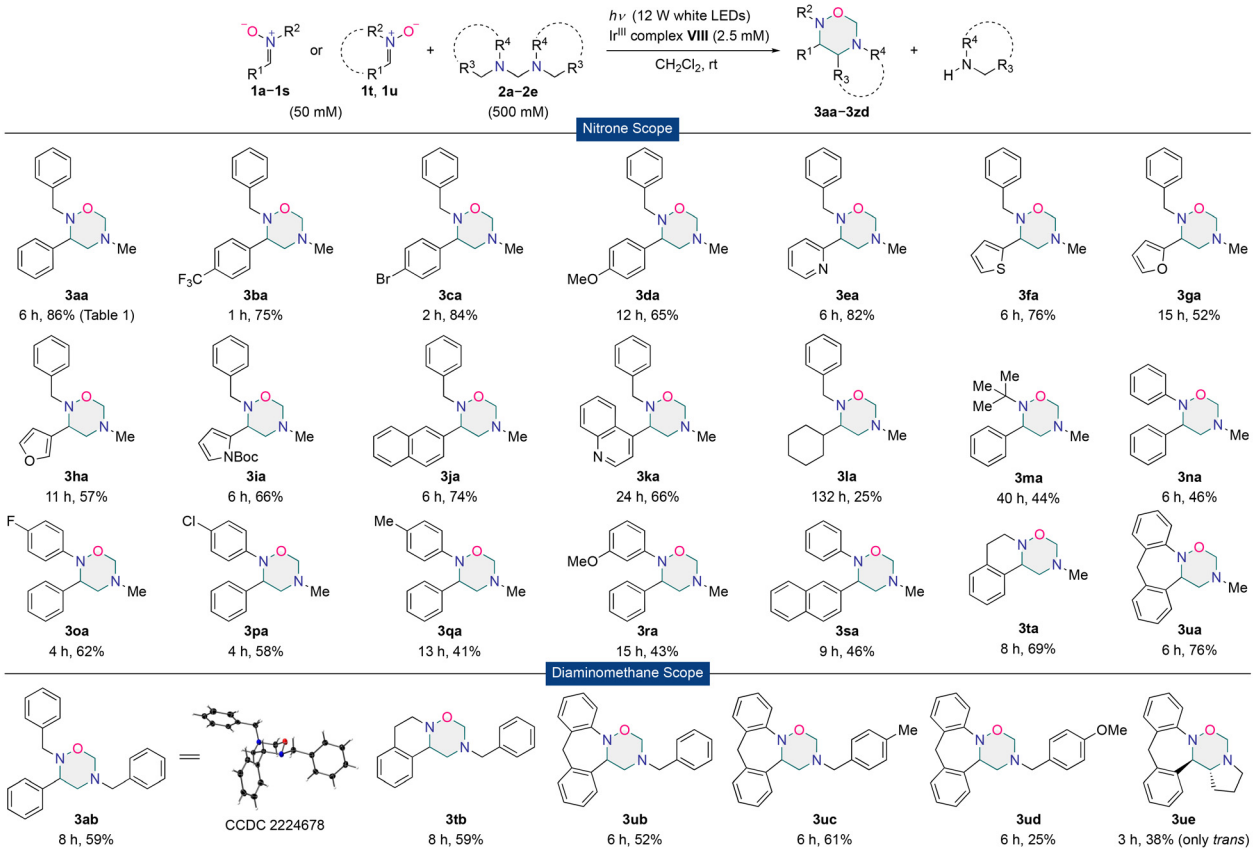

Scheme 2 Scope of nitrones and *N*,*N*,*N*′,*N*′-tetraalkyldiaminomethanes. Reaction conditions: nitrone **1** (50 mM), *N*,*N*,*N*′,*N*′-tetraalkyldiaminomethane **2** (500 mM), and Ir^{III} complex **VIII** (2.5 mM) in CH_2Cl_2, irradiated using the LED strip (λ = 400–780 nm, 12 W, 60 white LEDs per m). All products were isolated.

Mechanistic study

To elucidate the reaction mechanism of the formal [3 + 3] photocyclization, we conducted quenching experiments on Ir^{III} complex **VIII**. The emission of **VIII** was attenuated upon addition of **1a** and **2a**, yielding Stern–Volmer plots (Scheme 3a) and uncovering Stern–Volmer constants (K_{SV}) of 1.01×10^4 M^{-1} for **1a** and 2.86×10^3 M^{-1} for **2a**. Notably, the molar concentration of **2a** (500 mM) was 10-times higher than that of **1a** (50 mM), resulting in a quenching efficiency ratio of 1 : 2.8 for K_{SV} [**1a**] : K_{SV} [**2a**]. This finding suggests that the quenching biases **2a** rather than **1a**. Deaerated CH_2Cl_2 was essential,

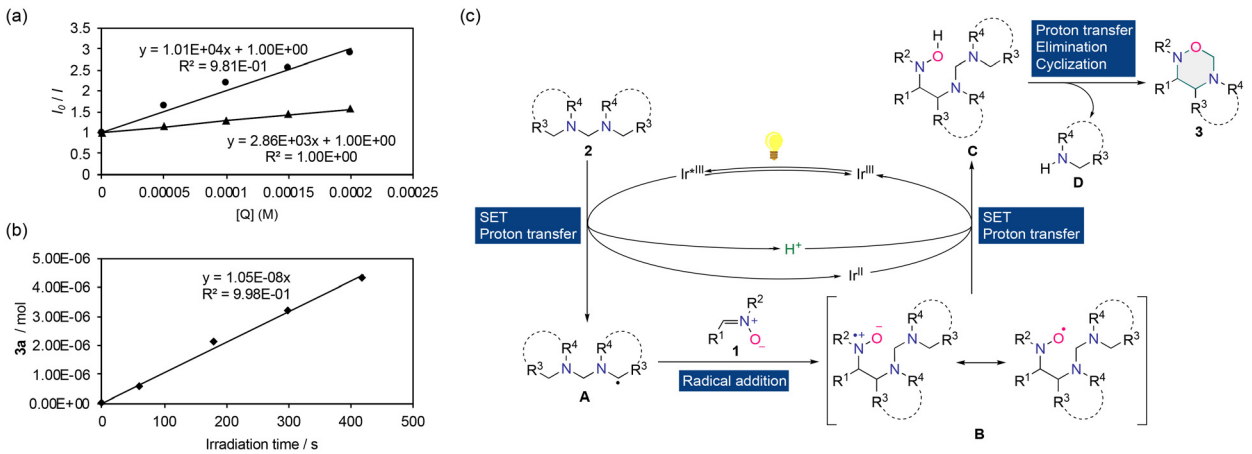

Scheme 3 (a) Quenching Ir^{III} complex **VIII** (4.00×10^{-6} M in CH_2Cl_2) emission by adding quencher (Q) **1a** (●) and **2a** (▲). (b) The rate of formation of product (**3aa**) in the reaction of **1a** (50 mM) with **2a** (500 mM) in the presence of **VIII** (2.5 mM) in CH_2Cl_2. (c) A plausible mechanism for the photocycloaddition.

indicating that the reaction requires the triplet excited state of **VIII**. Subsequently, the quantum yield for the formation of **3aa** (Φ_{3aa}) was determined by dividing the rate of **3aa** formation (1.05×10^{-8} mol s^{-1}) by the rate of Fe(II) production (4.63×10^{-8} Einsteins s^{-1}) during the photolysis of $K_3[Fe(C_2O_4)_3]$,[38,39] resulting in a value of 0.23 (Scheme 3b). As the quantum yield was less than 1.00, we excluded the non-photochemical radical chain mechanism. We updated the data for the photophysical properties of **VIII** due to an unclear $E_{1/2}$ (Ir^{III}/Ir^{II}) value in our previous study.[40] Therefore, we further scrutinized the cyclic voltammetry conditions in analyzing **VIII** and determined the electrochemical potentials for the ground state of Ir^{III} complex **VIII** [E^c (Ir^{III}/Ir^{II}) = −1.26 V *versus* Fc/Fc^+ in CH_3CN; E^a (Ir^{III}/Ir^{IV}) = +1.30 V *versus* Fc/Fc^+ in CH_3CN]. The 0–0 transition frequency of **VIII** was reported previously to be 2.67 V.[40] Thus, the excited state potential of Ir^{III} complex **VIII*** can be calculated as E^* (Ir^{*III}/Ir^{II}) = +1.41 V *versus* Fc/Fc^+ in CH_3CN and E^* (Ir^{*III}/Ir^{IV}) = −1.37 V *versus* Fc/Fc^+ in CH_3CN. The potential of **2a** [E_p^a (**2a**/**2a**$^{\bullet+}$) = +0.52 V *versus* Fc/Fc^+ in CH_3CN] was reported previously.[40] We observed that the electrochemical potential of **1a** ranged from −1.60 V to +1.70 V *versus* Fc/Fc^+ in CH_3CN, consistent with the reported potentials of (*Z*)-*N*-(phenylmethylene)methanamine *N*-oxide.[41] The triplet energies of **VIII** and **1a** are within a narrow range, noted at 2.67 eV (ref. 40) and 2.0 eV,[42] respectively. This suggests the feasibility of energy transfer between the photoexcited **VIII** and the ground state **1a**, and potentially leads to the decomposition of **1a** under suitable conditions. However, in the absence of **2a**, no decomposition of **1a** occurred in the presence of **VIII** under visible-light irradiation (λ = 400–780 nm), indicating that energy transfer did not occur. Considering the electron transfer between **1a** and the Ir species,[43a,b] it is conceivable that this process is reversible in our investigation, consistent with the findings of those who developed and elucidated the [3 + 3] dipolar cycloaddition of nitrones with aryl cyclopropanes *via* visible-light acridinium-based organophotoredox catalysis.[43b]

Based on these findings, we propose a plausible reaction mechanism in Scheme 3c. The ground state Ir^{III} complex (Ir^{III}) absorbs light to generate the photoexcited Ir^{III} complex (Ir^{*III}), which oxidizes **2** *via* SET, followed by proton transfer to generate the α-aminoalkyl radical **A** and the ground state Ir^{II} complex (Ir^{II}). α-Aminoalkyl radical **A** is generated in a regioselective manner based on a stereoelectronic rule.[44,45] Nitrone **1** traps **A** to form the resonance-stabilized radical **B**. Subsequently, **B** receives an electron from the ground state Ir^{III} and a proton, yielding *N*-benzylhydroxylamine **C** and regenerating the ground state Ir^{III}. *N*-Benzylhydroxylamine **C** then cyclizes, accompanied by proton transfer to one of the tertiary amine nitrogens, releasing the secondary amine **D**.

Flow synthesis and derivatization

To achieve multi-gram-scale synthesis of a target molecule in drug discovery, we developed the photochemical flow reactor and applied it to the reaction of **1t** (11.6 mmol) with **2b** (Scheme 4). The reaction proceeded smoothly, yielding

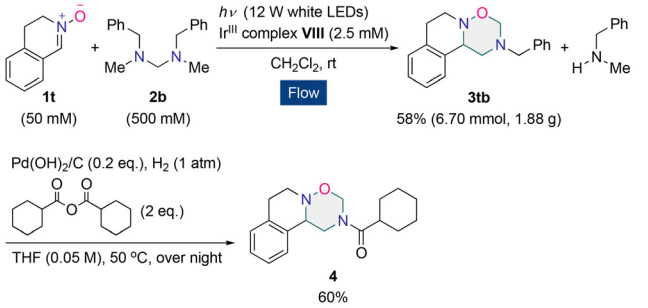

Scheme 4 Gram-scale photoflow synthesis of **3tb** and preparation of **4**. LED tape length, 4 m (60 LEDs per m); PTFE tube O.D. 1.59 mm, I.D. 0.8 mm, 3.75 m; average flow rate 0.0420 mL min^{-1}; total amount of liquid fed, 231 mL; residence time, 45 min.

1.88 g (6.70 mmol) of **3tb** in a single photochemical flow operation (Fig. S2†). Subsequently, we employed 518 mg (1.85 mmol) of **3tb** for acylative debenzylation in the presence of cyclohexanecarboxylic anhydride, $Pd(OH)_2/C$, under a hydrogen atmosphere, thereby completing the synthesis of **4**.

Biological activity

Our ongoing investigation focused on evaluating and comparing the *anti*-schistosomal activities of **4** and PZQ against *Schistosoma mansoni* (Table 2; see ESI† for videos of the worm movement). Remarkably, **4** exhibited comparable activity and a rapid onset of action against adult worms. Marchant and colleagues have conducted meticulous research to elucidate the interaction of PZQ with the transient receptor potential ion channel of the melastatin subfamily of *S. mansoni*, *Sm*. $TRPM_{PZQ}$.[46] According to their recent findings, the piperazin-2-one carbonyl of PZQ forms a crucial hydrogen bond with *Sm*. $TRPM_{PZQ}$, contributing to binding energy.[46b] Therefore, the remarkable biological activity of **4** is particularly surprising, as it lacks this essential functional group.

ADMET property

Next, we comprehensively assessed the melting point, solubility, membrane permeability, stability under acidic pH, and metabolic stability of **4** to evaluate its potential as a lead compound in the discovery of a new chemotype demonstrating an *anti*-schistosomal effect (Table 3). Comparing the melting points of PZQ[13] and **4**, we noted that 4 exhibited a significantly lower melting point, indicating weaker molecular packing.[3a,d,g,47,48] The log *D* value of PZQ could not be estimated due to its limited solubility in phosphate-buffered saline (PBS) at pH 7.4. In contrast, **4**, a new chemotype, demonstrated sufficient solubility in PBS, yielding a favorable value of 4.1, which is suitable for oral administration.[49] Consequently, **4** is expected to have enhanced solubility in PBS at pH 7.4. Conversely, due to its significantly low solubility, PZQ was not detected in high-performance liquid chromatography with ultraviolet detection.[13,21] To elucidate the notable solubility of **4**, we assessed its molecular polarity by calculating the dipole moments of both PZQ and **4** (Fig. S6†).[50] These computational

Table 2 Comparison of the biological efficacy of **4** and PZQ against *S. mansoni*[a]

Compound[b]	Motility and survival of the worms[c,d,e]					
	Adult (♂)			Adult (♀)		
	1 h	24 h	120 h	1 h	24 h	120 h
PZQ	3.7	3.7	3.3	3.7	3.3	3.3
4	3.0	3.0	3.0	2.0	2.0	2.3
None[f]	0	0	0	0	0	0

[a] Mice were inoculated with approximately 250 cercariae and underwent a 6-week incubation period. Subsequently, the mice were euthanized to harvest the adult schistosomes from the mesenteric veins using tweezers or by perfusion. All procedures were performed in compliance with the ethical guidelines of the Kitasato University Animal Experiment Ethics Committee (approval no. 2022-074, 2023-123). [b] The molar concentration of compounds was 10 μM. [c] The motility and survival of the worms were evaluated based on a 0 to 4 viability scale: 0 indicated full motility with worms adherent to the well bottom; 1 indicated partial detachment with weak movement; 2 represented full detachment with weak movement; 3 was characterized by no pairing and varied movement intensity, or no movement but still alive; 4 denoted deceased worms. A treatment was deemed lethal if no worm movement was observed for 1 minute. Data are presented as the mean of three independent experiments. [d] The health status of the adult worms, including their motility and mortality, was assessed using an inverted microscope. [e] Post-treatment, the parasites were monitored daily for 5 days (120 hours). [f] DMSO served as the vehicle control.

studies were performed using the B3LYP hybrid functional and a 6-31G** basis set within Gaussian16.[51] The solvent effects of water were considered using the polarizable continuum model with the integral equation formalism variant (IEFPCM). The computations yielded dipole moment values of 1.97 debye for PZQ and 3.96 debye for **4**. The dipole moment value of **4** was significantly larger than that of PZQ, corroborating its substantially greater solubility in polar solvents compared to PZQ. In permeability studies employing the Caco-2 cell assay, **4** demonstrated adequate permeability through human epithelial cells.[22a,52,53] Evaluation of its stability under acidic pH revealed resilience despite the presence of the *N*,*O*-acetal structure. We then investigated the metabolic stability of both PZQ and **4** in liver microsomes. Although PZQ underwent faster metabolism than expected,[23a] **4** exhibited even greater attenuation than PZQ, in contrast to our initial expectations.

We also performed a cell viability assay in HeLa cells and found no detrimental effects when comparing **4** and PZQ (Fig. 1a). Furthermore, we performed a cardiac safety assay using human induced pluripotent stem cell (iPSC)-derived cardiomyocytes, iCell® Cardiomyocytes[2],[54] to compare the cardiotoxic effects of **4** with those of PZQ. PZQ and **4** were added to cardiomyocytes, and the resulting calcium ion influx was monitored using a fluorescent indicator. This process generated calcium (Ca^{2+}) oscillation profiles (Fig. 1b). The Ca^{2+} flux signal in each well provided a view of the beating profiles of the cardiac cells over 20 seconds for both untreated cells and cells treated with PZQ or **4**. The peak height (amplitude) represents the maximum change in calcium flux during a cardiac cycle; a higher peak amplitude suggests stronger contraction of the cardiac cells, whereas a lower peak amplitude indicates weaker contraction. The peak width represents the duration of the calcium transient. A broader peak indicates longer duration of calcium presence, suggesting prolonged contraction or slower relaxation of the cardiomyocytes. Conversely, a narrower peak indicates a shorter contraction time or quicker relaxation. These metrics provide valuable insights into the timing of the cardiac cycle and are crucial for evaluating the potential of compounds to prolong the QT-interval, which is associated with the onset of arrhythmias. We evaluated the impact of E-4031, a known human ether-a-go-go-related gene (hERG) channel blocker, as a positive control, which induced significant cardiac toxicity (Fig. S8†).[55,56] Upon addition of PZQ at various concentrations (0.2 μM, 2 μM, 20 μM), no changes in the pulse waveforms or beat intervals were observed within the 60 minutes before and after addition. In contrast, the addition of 20 μM of **4** did not alter the pulse waveforms, but resulted in shortened beat intervals for 60 minutes. At 2 μM of **4**, the pulse waveforms remained unchanged, but a slight shortening of beat intervals was observed for up to 30 minutes post-addition, eventually reverting to the pre-addition state within 60 minutes (Fig. S9†).

Table 3 Comparing log *D*, melting point, solubility, membrane permeability, stability under acidic pH, and metabolic stability of **4** *versus* PZQ

Comp.	M.p. (°C)	log *D*[a]	Sol.[a]	Caco-2 cell permeability[b]		Remaining ratio (%) in acidic and neutral media[c]				Remaining ratio (%) in liver microsomes			
						pH 1.2		pH 7.4		Human		Mouse	
				Papp	Class	1 h	5 h	1 h	5 h	10 min	60 min	10 min	60 min
PZQ	136–138[d]	N.E.[e]	N.D.[f,g]	37.3	High	93.1	95.0	103.2	100.1	87.5	49.8	11.5	0.1
4	106–107	4.1	≧95	30.5	High	95.1	94.9	95.2	93.3	47.3	5.9	2.7	0.2

[a] PBS (pH 7.4) was used as the buffer. [b] Employing a well-established method demonstrated in ref. 53 that measured the rate of flux of compounds across polarized Caco-2 cell monolayers (Papp: × 10^{-6} cm s). [c] A disintegration testing instrument and conditions were utilized for the evaluation. [d] Reported value in ref. 13. [e] N.E. stands for "not estimated". [f] N.D. stands for "not detected". [g] Insoluble in water.

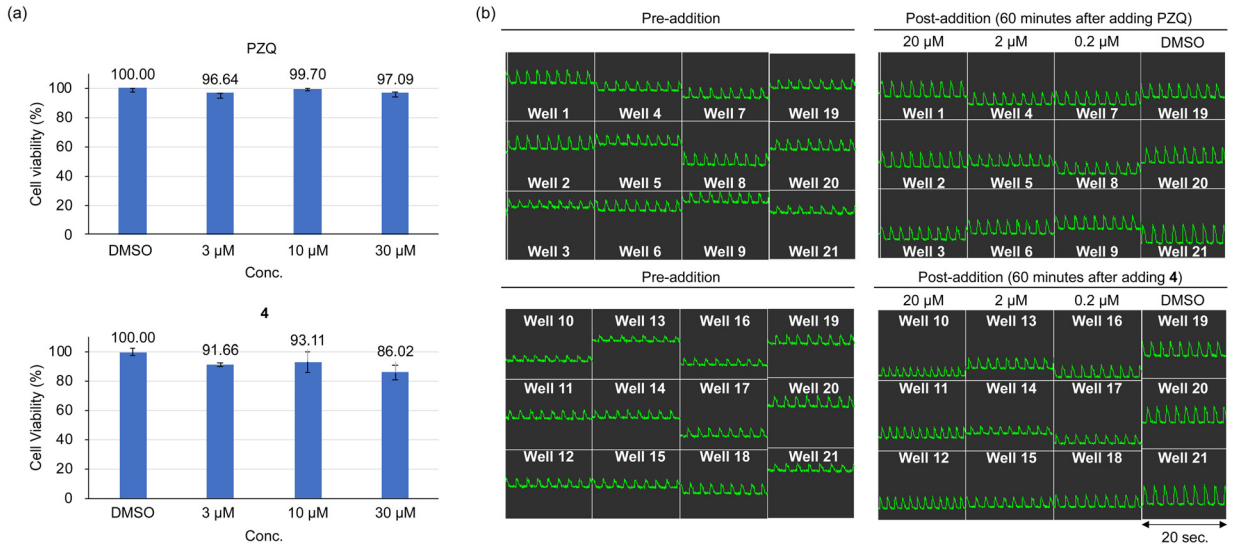

Fig. 1 (a) The cell viability assay was performed by treating HeLa cells with solutions of PZQ and **4** in DMSO, followed by addition of WST-8 [2-(2-methoxy-4-nitrophenyl)-3-(4-nitrophenyl)-5-(2,4-disulfophenyl)-2*H*-tetrazolium, monosodium salt] after 48 hours and measuring absorbance at 450 nm. Error bars are indicated for each result. (b) In the cardiac safety assay, each peak corresponds to the contraction of cardiomyocytes detected through the influx of calcium ions into the cardiomyocytes using the fluorescent indicator (EarlyTox™ Cardiotoxicity kit) and depicted based on its fluorescence intensity. Solutions of PZQ and **4** in DMSO were tested with three samples for each concentration (n = 3): wells 1, 2, and 3 for 20 μM PZQ; wells 4, 5, and 6 for 2 μM PZQ; wells 7, 8, and 9 for 0.2 μM PZQ; wells 10, 11, and 12 for 20 μM **4**; wells 13, 14, and 15 for 2 μM **4**; wells 16, 17, and 18 for 0.2 μM **4**; wells 19, 20, and 21 for DMSO.

The addition of 0.2 μM of **4** did not affect the pulse waveforms and beat intervals for 60 minutes. Notably, there were no signs of QT-interval prolongation, early after-depolarization, or cardiomyocyte cell cycle arrest. Thus, we concluded that both compounds exhibit potential liabilities to cardiovascular safety.

Conclusions

Our investigation into replacing the piperazin-2-one ring of PZQ with a 1,2,5-oxadiazinane ring successfully identified a novel chemotype with highly potent *anti*-schistosomal activity. This derivative demonstrates significant efficacy against *S. mansoni* while largely preserving the potent biological activity of the parent compound. Notable attributes include excellent solubility, resilience to acid exposure, and potential liabilities to cardiovascular safety and cell viability. These results advocate for the 1,2,5-oxadiazinane moiety as a bioisostere of piperazin-2-one. Our ongoing efforts are focused on enhancing the metabolic stability of this molecule and conducting further structure–activity relationship studies to surpass the efficacy of PZQ. Our exploration of bioisosteric replacement and the discovery of this *anti*-schistosomal molecule were facilitated by our pivotal synthetic methodology involving the formal [3 + 3] photocycloaddition reaction between nitrones and *N*,*N*,*N*′,*N*′-tetraalkyldiaminomethanes, yielding a diverse array of 1,2,5-oxadiazinane structures. Utilizing a photochemical flow reactor, we achieved multi-gram-scale synthesis of an intermediate for the target molecule, which is crucial for drug discovery. The proposed mechanism for the photocycloaddition is convincing and opens new avenues for synthesizing novel saturated nitrogen-containing heterocycles that are potentially useful in bioisosteric replacement.

Data availability

The data supporting this study's findings are available in the ESI† of this article. Videos for the worm movement assay are also included.

Author contributions

K. I. conceived the research, executed the experiments, analyzed the data, wrote the manuscript, and supervised the project; H. N. synthesized the *anti*-schistosomal molecule, optimized the photocycloaddition, and developed the photoflow synthesis; A. K. optimized the photoflow synthesis; A. T. and Y. A. optimized the photocycloaddition; A. H. carried out the kinetic experiments to determine the quantum yield and Stern–Volmer constants; T. M., F. K., and S. H. provided valuable advice to advance the research; K. N. and R. S. conducted SCXRD, HRMS, and FAB-MS analyses; N. S. performed NMR experiments; K. O. and M. H. conducted emission experiments at 77 K and elemental analysis; K. T. executed the computational study; H. I. synthesized Ru^{II} complexes and provided helpful advice for photochemistry experiments; F. M., K. D. K., H. K., T. H., and N. T. performed and evaluated the worm movement assays and provided valuable information on advanced Schistosomiasis research; B. L., K. N., T. K., and J. H. not only performed and evaluated ADMET assays and provided guidance on drug discovery in the pharmaceutical industry; H. F. provided fruitful

advice on the medicinal chemistry research in academia and pharmaceutical industry and supervised the project.

Conflicts of interest

There are no conflicts to declare.

Acknowledgements

This research was supported by Research Support Project for Life Science and Drug Discovery (Basis for Supporting Innovative Drug Discovery and Life Science Research (BINDS)) from AMED under grant number JP24ama121054.

Notes and references

1 C. M. Marson, *Adv. Heterocycl. Chem.*, 2017, **121**, 13–33.
2 H. Chen, O. Engkvist and T. Kogej, in *The Practice of Medicinal Chemistry*, ed. C.G. Wermuth, D. Aldous, P. Raboisson and D. Rogan, Academic Press, London, 4th edn, 2015, pp. 384–385.
3 (*a*) F. Lovering, J. Bikker and C. Humblet, *J. Med. Chem.*, 2009, **52**, 6752–6756; (*b*) G. Wuitschik, E. M. Carreira, B. Wagner, H. Fischer, I. Parrilla, F. Schuler, M. Rogers-Evans and K. Müller, *J. Med. Chem.*, 2010, **53**, 3227–3246; (*c*) N. A. Meanwell, *J. Med. Chem.*, 2011, **54**, 2529–2591; (*d*) F. Lovering, *Med. Chem. Commun.*, 2013, **4**, 515–519; (*e*) R. D. Taylor, M. MacCoss and A. D. G. Lawson, *J. Med. Chem.*, 2014, **57**, 5845–5859; (*f*) E. Vitaku, D. T. Smith and J. T. Njardarson, *J. Med. Chem.*, 2014, **57**, 10257–10274; (*g*) W. Wei, S. Cherukupalli, L. Jing and X. Liu, *Drug Discovery Today*, 2020, **25**, 1839–1845; (*h*) M. A. M. Subbaiah and N. A. Meanwell, *J. Med. Chem.*, 2021, **64**, 1839–1845; (*i*) N. A. Meanwell and O. Loiseleur, *J. Agric. Food Chem.*, 2022, **70**, 10942–10971; (*j*) N. A. Meanwell and O. Loiseleur, *J. Agric. Food Chem.*, 2022, **25**, 1839–1845.
4 (*a*) O. Méndez-Lucio and J. L. Medina-Franco, *Drug Discovery Today*, 2017, **22**, 120–126; (*b*) W. Wei, S. Cherukupalli, L. Jing, X. Liu and P. Zhan, *Drug Discovery Today*, 2020, **22**, 120–126; (*c*) J. Shearer, J. L. Castro, A. D. G. Lawson, M. MacCoss and R. D. Taylor, *J. Med. Chem.*, 2022, **65**, 8699–8712.
5 (*a*) G. Wuitschik, M. Rogers-Evans, A. Buckl, M. Bernasconi, M. Märki, T. Godel, H. Fischer, B. Wagner, I. Parrilla, F. Schuler, J. Schneider, A. Alker, W. B. Schweizer, K. Müller and E. M. Carreira, *Angew. Chem., Int. Ed.*, 2008, **47**, 4512–4515; (*b*) J. A. Burkhard, B. Wagner, H. Fischer, F. Schuler, K. Müller and E. M. Carreira, *Angew. Chem., Int. Ed.*, 2010, **49**, 3524–3527; (*c*) J. A. Burkhard, G. Wuitschik, M. Rogers-Evans, K. Müller and E. M. Carreira, *Angew. Chem., Int. Ed.*, 2010, **49**, 9052–9067; (*d*) J. A. Burkhard, C. Guérot, H. Knust, M. Rogers-Evans and E. M. Carreira, *Org. Lett.*, 2010, **12**, 1944–1947; (*e*) C. Guérot, B. H. Tchitchanov, H. Knust and E. M. Carreira, *Org. Lett.*, 2011, **13**, 780–783.
6 (*a*) A. P. Mityuk, A. V. Denisenko, O. P. Dacenko, O. O. Grygorenko, P. K. Mykhailiuk, D. M. Volochnyuk, O. V. Shishkin and A. A. Tolmachev, *Synthesis*, 2010, 493–497; (*b*) A. V. Denisenko, A. P. Mityuk, O. O. Grygorenko, D. M. Volochnyuk, O. V. Shishkin, A. A. Tolmachev and P. K. Mykhailiuk, *Org. Lett.*, 2010, **12**, 4372–4375; (*c*) A. A. Kirichok, I. Shton, M. Kliachyna, I. Pishel and P. K. Mykhailiuk, *Angew. Chem., Int. Ed.*, 2017, **56**, 8865–8869; (*d*) B. A. Chalyk, M. V. Butko, O. O. Yanshyna, K. S. Gavrilenko, T. V. Druzhenko and P. K. Mykhailiuk, *Chem. – Eur. J.*, 2017, **23**, 16782–16786; (*e*) V. V. Levterov, O. Michurin, P. O. Borysko, S. Zozulya, I. V. Sadkova, A. A. Tolmachev and P. K. Mykhailiuk, *J. Org. Chem.*, 2018, **83**, 14350–14361; (*f*) A. A. Kirichok, I. O. Shton, I. M. Pishel, S. A. Zozulya, P. O. Borysko, V. Kubyshkin, O. A. Zaporozhets, A. A. Tolmachev and P. K. Mykhailiuk, *Chem. – Eur. J.*, 2018, **24**, 5444–5449; (*g*) D. Dibchak, M. Snisarenko, A. Mishuk, O. Shablykin, L. Bortnichuk, O. Klymenko-Ulianov, Y. Kheylik, I. V. Sadkova, H. S. Rzepa and P. K. Mykhailiuk, *Angew. Chem., Int. Ed.*, 2023, **62**, e202304246; (*h*) A. A. Kirichok, H. Tkachuk, Y. Kozyriev, O. Shablykin, O. Datsenko, D. Granat, T. Yegorova, Y. P. Bas, V. Semirenko, I. Pishel, V. Kubyshkin, D. Lesyk, O. Klymenko-Ulianov and P. K. Mykhailiuk, *Angew. Chem., Int. Ed.*, 2023, **62**, e202311583; (*i*) A. Denisenko, P. Garbuz, N. M. Voloshchuk, G. Al-Maali, P. Borysko and P. K. Mykhailiuk, *Nat. Chem.*, 2023, **15**, 1155–1163; (*j*) V. V. Levterov, Y. Panasiuk, K. Sahun, O. Stashkevych, V. Badlo, O. Shablykin, I. Sadkova, L. Bortnichuk, O. Klymenko-Ulianov, Y. Holota, L. Lachmann, P. Borysko, K. Horbatok, I. Bodenchuk, Y. Bas, D. Dudenko and P. K. Mykhailiuk, *Nat. Commun.*, 2023, **14**, 5608.
7 (*a*) C.-V. T. Vo, G. Mikutis and J. W. Bode, *Angew. Chem., Int. Ed.*, 2013, **52**, 1705–1708; (*b*) C.-V. T. Vo, M. U. Luescher and J. W. Bode, *Nat. Chem.*, 2014, **6**, 310–314; (*c*) W.-Y. Siau and J. W. Bode, *J. Am. Chem. Soc.*, 2014, **136**, 17726–17729; (*d*) C.-V. T. Vo and J. W. Bode, *J. Org. Chem.*, 2014, **79**, 2809–2815; (*e*) M. U. Luescher, K. Geoghegan, P. L. Nichols and J. W. Bode, *Aldrichimica Acta*, 2015, **48**, 43–48; (*f*) M. U. Luescher and J. W. Bode, *Org. Lett.*, 2016, **18**, 2652–2655; (*g*) Y. Wang and J. W. Bode, *J. Am. Chem. Soc.*, 2019, **141**, 9739–9745; (*h*) M. K. Škopić, F. Losch, A. E. McMillan, N. Willeke, M. Malenica, L. Bering, J. Bode and A. Brunschweiger, *Org. Lett.*, 2022, **24**, 1383–1387; (*i*) J. Götz, M. K. Jackl, C. Jindakun, A. N. Marziale, J. André, D. J. Gosling, C. Springer, M. Palmieri, M. Reck, A. Luneau, C. E. Brocklehurst and J. W. Bode, *Sci. Adv.*, 2023, **9**, eadj2314.
8 (*a*) M. Yar, E. M. McGarrigle and V. K. Aggarwal, *Angew. Chem., Int. Ed.*, 2008, **47**, 3784–3786; (*b*) M. G. Unthank, B. Tavassoli and V. K. Aggarwal, *Org. Lett.*, 2008, **10**, 1501–1504; (*c*) M. Yar, E. M. McGarrigle and V. K. Aggarwal, *Org. Lett.*, 2009, **11**, 257–260; (*d*) S. P. Frintz, T. H. West, E. M. McGarrigle and V. K. Aggarwal, *Org. Lett.*, 2012, **14**, 6370–6373; (*e*) S. P. Frintz, J. V. Matlock, E. M. McGarrigle and V. K. Aggarwal, *Chem. – Eur. J.*, 2013, **19**, 10827–10831; (*f*) J. A. Matlock, T. D. Svejstrup, P. Songara, S. Overington, E. M. McGarrigle and V. K. Aggarwal, *Org. Lett.*, 2015, **17**, 5044–5047; (*g*) A. Fawcett, A. Murtaza, C. H. U. Gregson and V. K. Aggarwal, *J. Am. Chem. Soc.*, 2019, **141**, 4573–4578; (*h*) J. L. Tyler, A. Noble and V. K. Aggarwal, *Angew. Chem., Int. Ed.*, 2021, **60**, 11824–11829; (*i*) J. L. Tyler, A. Noble and V. K. Aggarwal, *Angew. Chem., Int. Ed.*, 2022, **61**, e202114235.

9 (*a*) K. E. Gettys, Z. Ye and M. Dai, *Synthesis*, 2017, **49**, 2589–2604; (*b*) Z. Ye, S. Adhikari, Y. Xia and M. Dai, *Nat. Commun.*, 2018, **9**, 721.

10 A. V. Chernykh, A. N. Tkachenko, I. O. Feskov, C. G. Daniliuc, N. A. Tolmachova, D. M. Volochnyuk and D. S. Radchenko, *Synthesis*, 2016, **27**, 1824–1827.

11 Z. Dobi, T. Holczbauer and T. Soós, *Eur. J. Org. Chem.*, 2017, 1391–1395.

12 A. J. Boddy, D. P. Affron, C. J. Cordier, E. L. Rivers, A. C. Spivey and J. A. Bull, *Angew. Chem., Int. Ed.*, 2019, **58**, 1458–1462.

13 H. I. El-Subbagh and A. A. Al-Badr, in *Analytical Profiles of Drug Substances and Excipients*, ed. H. G. Brittain, Academic Press, San Diego, 1998, vol. 25, pp. 463–500; The Merck Index Online. "Praziquantel", can be found under **https://merckindex.rsc.org/monographs/m9107** (accessed 26 April 2024).

14 C. R. Caffrey, N. El-Sakkary, P. Mäder, R. Krieg, K. Becker, M. Schlitzer, D. H. Drewry, J. L. Vennerstrom and C. G. Grevelding, in *Neglected Tropical Dieaes: Drug Discovery and Development*, ed. D. C. Swinney, M. P. Pollastri, R. Mannhold, H. B. Buschmann and J. Holenz, Wiley-VCH Verlag GmbH & Co. KGaA., 2019, vol. 77, pp. 187–299.

15 (*a*) P. Andrews, H. Thomas, R. Pohlke and J. Seubert, *Med. Res. Rev.*, 1983, **3**, 147–200; (*b*) A. G. P. Ross, P. B. Bartley, A. C. Sleigh, G. R. Olds, Y. Li, G. M. Williams and D. P. McManus, *N. Engl. J. Med.*, 2002, **346**, 1212–1220; (*c*) D. P. McManus, D. W. Dunne, M. Sacko, J. Utzinger, B. J. Vennervald and X. N. Zhou, *Nat. Rev. Dis.*, 2018, **4**, 13; (*d*) C. M. Thomas and D. J. Timison, *Curr. Top. Med. Chem.*, 2018, **18**, 1575–1584; (*e*) S.-K. Park and J. S. Marchant, *Trends Parasitol.*, 2020, **36**, 182–194; (*f*) N. C. Lo, F. S. M. Bezerra, D. G. Colley, F. M. Fleming, M. Homeida, N. Kabatereine, F. M. Kabole, C. H. King, M. A. Mafe, N. Midzi, F. Mutapi, J. R. Mwanga, R. M. R. Ramzy, F. Satrija, J. R. Stothard, M. S. Traoré, J. P. Webster, J. Utzinger, X.-N. Zhou, A. Danso-Appiah, P. Eusebi, E. S. Loker, C. O. Obonyo, R. Quansah, S. Liang, M. Vaillant, M. H. Murad, P. Hagan and A. Garba, *Lancet Infect. Dis.*, 2022, **22**, e327–e335.

16 A. Wiesner, M. Skrońska, G. Gawlik, M. Marcinkowska, P. Zagrodzki and P. Paśko, *Aids Behav.*, 2023, **27**, 1441–1468.

17 N. Brown, in *Bioisosteres in Medicinal Chemistry*, ed. N. Brown, Wiley-VCH, Weinheim, 1st edn, 2012, pp. 3–29; D. A. Smith and D. S. Millan, in *Bioisosteres in Medicinal Chemistry*, ed. N. Brown, Wiley-VCH, Weinheim, 1st edn, 2012, pp. 31–51; P. Ciapetti and B. Giethlen, in *The Practice of Medicinal Chemistry*, ed. C. G. Wermuth, D. Aldous, P. Raboisson and D. Rogan, Academic Press, London, 4th edn, 2015, pp. 181–220.

18 (*a*) G. A. Patani and E. J. LaVoie, *Chem. Rev.*, 1996, **96**, 3147–3176; (*b*) N. A. Meanwell, *J. Med. Chem.*, 2011, **54**, 2529–2591; (*c*) N. Brown, *Mol. Inf.*, 2014, **33**, 458–462; (*d*) N. A. Meanwell, *J. Agric. Food Chem.*, 2023, **71**, 18087–18122.

19 M. Lindenberg, S. Kopp and J. B. Dressmana, *Eur. J. Pharm. Biopharm.*, 2004, **58**, 265–278.

20 (*a*) F. Ronketti, A. V. Ramana, X. C. Ming, L. Pica-Mattoccia, D. Ciolic and M. H. Todd, *Bioorg. Med. Chem. Lett.*, 2007, **17**, 4154–4157; (*b*) W.-L. Wang, L.-J. Song, X. Chen, X.-R. Yin, W.-H. Fan, G.-P. Wang, C.-X. Yu and B. Feng, *Molecules*, 2013, **18**, 9163–9178; (*c*) M. Patra, K. Ingram, A. Leonidova, V. Pierroz, S. Ferrari, M. N. Robertson, M. H. Todd, J. Keiser and G. Gasser, *J. Med. Chem.*, 2013, **56**, 9192–9198; (*d*) Z.-X. Wang, J.-L. Chen and C. Qiao, *Chem. Biol. Drug Des.*, 2013, **82**, 216–225; (*e*) Y. Zheng, L. Dong, C. Hu, B. Zhao, C. Yang, C. Xia and D. Sun, *Bioorg. Med. Chem. Lett.*, 2014, **24**, 2481–2484.

21 I. D'Abbrunzo, G. Procida and B. Perissutti, *Pharmaceutics*, 2024, **16**, 27–38.

22 (*a*) G.-E. Dinora, R. Julio, C. Nelly, Y.-M. Lilian and H. J. Cook, *Int. J. Pharm.*, 2005, **295**, 93–99; (*b*) N. El-Lakkany, S. H. S. El-Din and L. Heikal, *Eur. J. Drug Metab. Pharmacokinet.*, 2012, **37**, 289–299; (*c*) A. D. A. Silva, M. A. Sarcinelli, B. F. C. Patricio, M. H. C. Chaves, L. M. Lima, P. M. Parreiras, P. F. Pinto, L. D. Prado and H. V. A. Rocha, *J. Drug Deliv. Sci. Technol.*, 2023, **81**, 104260.

23 (*a*) N. Castro, R. Medina, J. Sotelo and H. Jung, *Antimicrob. Agents Chemother.*, 2000, **44**, 2903–2904; (*b*) P. Olliaro, P. Delgado-Romero and J. Keiser, *J. Antimicrob. Chemother.*, 2014, **69**, 863–870; (*c*) N. Abla, J. Keiser, M. Vargas, N. Reimers, H. Haas and T. Spangenberg, *PLoS Negl. Trop. Dis.*, 2017, **11**, e0005942.

24 T. Meyer, H. Sekljic, S. Fuchs, H. Bothe, D. Schollmeyer and C. Miculka, *PLoS Negl. Trop. Dis.*, 2009, **3**, e357.

25 "The Pediatric Praziquantel Consortium", can be found under **https://www.pediatricpraziquantelconsortium.org/**, 2024 (accessed 01 May 2024).

26 "European Medicines Agency (EMA) adopts a positive scientific opinion on arPraziquantel", can be found under **https://www.who.int/news/item/07-02-2024-european-medicines-agency-(ema)-adopts-a-positive-scientific-opinion-on-arpraziquantel**, 2024 (accessed 01 May 2024).

27 E. K. N'Goran, M. R. Odiere, R. A. Aka, M. Ouattara, N. A. D. Aka, B. Ogutu, F. Rawago, W. M. Bagchus, M. Bödding, E. Kourany-Lefoll, A. Tappert, X. Yin, D. Bezuidenhout, H. Badenhorst, E. Huber, B. Dälken and O. H.-A. Saflo, *Lancet Infect. Dis.*, 2023, **23**, 867–876.

28 D. J. Sprague, S.-K. Park, S. Gramberg, L. Bauer, C. M. Rohr, E. G. Chulkov, E. Smith, L. Scampavia, T. P. Spicer, S. Haeberlein and J. S. Marchant, *Nat. Struct. Mol. Biol.*, 2024, **31**, 1386.

29 (*a*) J. C. Espinosa-Lara, D. Guzman-Villanueva, J. I. Arenas-García, D. Herrera-Ruiz, J. Rivera-Islas, P. Romań-Bravo, H. Morales-Rojas and H. Höpfl, *Cryst. Growth Des.*, 2013, **13**, 169–185; (*b*) A. Borrego-Sánchez, C. Viseras, C. Aguzzi and C. I. Sainz-Díaz, *Eur. J. Pharm. Sci.*, 2016, **92**, 266–275.

30 V. B. R. Silva, B. R. K. L. Campos, J. F. Oliveira, J.-L. Decout and M. C. A. Lima, *Bioorg. Med. Chem.*, 2017, **25**, 3259–3277.

31 P. Ciapetti and B. Giethlen, in *The Practice of Medicinal Chemistry*, ed. C. G. Wermuth, D. Aldous, P. Raboisson and D. Rogan, Academic Press, London, 4th edn, 2015, p. 187, (Table 8.5).

32 (*a*) F. G. Riddell and E. S. Turner, *Tetrahedron*, 1979, **35**, 1311–1314; (*b*) K. Bell, M. P. Coogan, M. B. Gravestock, D. W. Knight and S. R. Thornton, *Tetrahedron Lett.*, 1997, **38**, 8545–8552; (*c*) K. K. Afanaseva, M. M. Efremova, S. V.

Kuznetsova, A. V. Ivanov, G. L. Starova and A. P. Molchanov, *Tetrahedron*, 2018, **74**, 5665–5673.

33 K. Itoh, A. Takashino, A. Ohtsuka, M. Kobe, S. Sawamura, R. Kato, S. Hirayama, F. Karaki, T. Mizuguchi, N. Sato, K. Tokunaga, Y. Toda, H. Suga, H. Ishida and H. Fujii, *ChemPhotoChem*, 2020, **4**, 388–392.

34 J. D. Wraver III and R. Overfield, in *Springer Handbook of Inorganic Photochemistry*, ed. D. W. Bahnemann and A. O. T. Patrocinio, Springer Nature Switzerland AG, 2022, pp. 1481–1508.

35 (*a*) K. Teegardin, J. I. Day, J. Chan and J. Weaver, *Org. Process Res. Dev.*, 2016, **20**, 1156–1163; (*b*) J. Zheng, X. Dong and T. P. Yoon, *Org. Lett.*, 2020, **22**, 6520–6525; (*c*) M. A. Bryden and E. Zysman-Colman, *Chem. Soc. Rev.*, 2021, **50**, 7587–7680; (*d*) J. Tang, L. Ren, J. Li, Y. Wang, D. Hu, X. Tong and C. Xia, *Org. Lett.*, 2022, **24**, 3582–3587; (*e*) N. Holmberg-Douglas and D. A. Nicewicz, *Chem. Rev.*, 2022, **122**, 1925–2016.

36 (*a*) X. Li, B. Minaev, H. Ågren and H. Tian, *Eur. J. Inorg. Chem.*, 2011, 2517–2524; (*b*) Y. Chen, C. Liu and L. Wang, *Tetrahedron*, 2019, **75**, 130686.

37 (*a*) C. K. Prier, D. A. Rankic and D. W. C. MacMillan, *Chem. Rev.*, 2013, **113**, 5322–5363; (*b*) K. Nakajima, Y. Miyake and Y. Nishibayashi, *Acc. Chem. Res.*, 2016, **49**, 1946–1956; (*c*) D. Staveness, I. Bosque and C. R. J. Stephenson, *Acc. Chem. Res.*, 2016, **49**, 2295–2306; (*d*) P. R. D. Murray, J. H. Cox, N. D. Chiappini, C. B. Roos, E. A. McLoughlin, B. G. Hejna, S. T. Nguyen, H. H. Ripberger, J. M. Ganley, E. Tsui, N. Y. Shin, B. Koronkiewicz, G. Qiu and R. R. Knowles, *Chem. Rev.*, 2022, **122**, 2017–2291.

38 M. Montalti, A. Credi, L. Prodi and M. T. Gandolfi, in *Handbook of Photochemistry*, CRC Press, Boca Raton, 3rd edn, 2006, pp. 601–616.

39 K. Itoh, S. Nagao, K. Tokunaga, S. Hirayama, F. Karaki, T. Mizuguchi, K. Nagai, N. Sato, M. Suzuki, M. Hashimoto and H. Fujii, *Chem. – Eur. J.*, 2021, **27**, 5171–5178.

40 K. Itoh, N. Ishii, A. Takashino, A. Hara, S. Kon, T. Mizuguchi, F. Karaki, S. Hirayama, Y. Shibagaki, K. Nagai, N. Sato, K. Tokunaga, M. Suzuki, M. Hashimoto and H. Fujii, *J. Photochem. Photobiol., A*, 2022, **434**, 114239.

41 P. H. R. Oliveira, É. A. Tordato, J. A. C. Vélez, P. S. Carneiro and M. W. Paixaõ, *J. Org. Chem.*, 2023, **88**, 6407–6419.

42 D. R. Cyr, T. Mathew, K. Ashok, P. K. Das and M. V. George, *J. Photochem. Photobiol., A*, 1991, **60**, 161–174.

43 (*a*) G. Haun, A. N. Paneque, D. W. Almond, B. E. Austin and G. Moura-Letts, *Org. Lett.*, 2019, **21**, 1388–1392; (*b*) Y. Xu, H.-X. Gao, C. Pan, Y. Shi, C. Zhang, G. Huang and C. Feng, *Angew. Chem., Int. Ed.*, 2023, **62**, e202310671.

44 F. D. Lewis, *Acc. Chem. Res.*, 1986, **19**, 401–405.

45 F. D. Lewis and T.-I. Ho, *J. Am. Chem. Soc.*, 1980, **102**, 1751–1752.

46 (*a*) S.-K. Park, G. S. Gunaratne, E. G. Chulkov, F. Moehring, P. McCusker, P. I. Dosa, J. D. Chan, C. L. Stucky and J. S. Marchant, *J. Biol. Chem.*, 2019, **294**, 18873–18880; (*b*) S.-K. Park, L. Friedrich, N. A. Yahya, C. M. Rohr, E. G. Chulkov, D. Maillard, F. Rippmann, T. Spangenberg and J. S. Marchant, *Sci. Transl. Med.*, 2021, **13**, eabj5832; (*c*) W. Le Clec'h, F. D. Chevalier, A. C. A. Mattos, A. Strickland, R. Diaz, M. McDew-White, C. M. Rohr, S. Kinung'hi, F. Allan, B. L. Webster, J. P. Webster, A. M. Emery, D. Rollinson, A. G. Djirmay, K. M. Al Mashikhi, S. Al Yafae, M. A. Idris, H. Moné, G. Mouahid, P. LoVerde, J. S. Marchant and T. J. C. Anderson, *Sci. Transl. Med.*, 2021, **13**, eabj9114; (*d*) C. M. Rohr, D. J. Spraguea, S.-K. Parka, N. J. Malcolma and J. S. Marchant, *Proc. Natl. Acad. Sci. U. S. A.*, 2023, **120**, e2217732120; (*e*) D. Sprague, M. Kaethner, S.-K. Park, C. M. Rohr, J. L. Harris, D. Maillard, T. Spangenberg, B. Lundström-Stadelmann and J. S. Marchant, *ACS Med. Chem. Lett.*, 2023, **14**, 1537–1543; (*f*) S.-K. Park, D. J. Sprague, C. M. Rohr, E. G. Chulkov, I. Petrow, S. Kumar and J. S. Marchant, *J. Biol. Chem.*, 2024, **300**, 105528.

47 M. Ishikawa and Y. Hashimoto, *J. Med. Chem.*, 2011, **54**, 1539–1554.

48 M. A. Walker, *Expert Opin. Drug Discovery*, 2014, **9**, 1421–1433.

49 (*a*) C. A. Lipinski, F. Lombardo, B. W. Dominy and P. J. Feeny, *Adv. Drug Delivery Rev.*, 1997, **23**, 3–25; (*b*) M. C. Wenlock, R. P. Austin, P. Barton, A. M. Davis and P. D. A. Leeson, *J. Med. Chem.*, 2003, **46**, 1250–1256; (*c*) M. J. Waring, *Expert Opin. Drug Discovery*, 2010, **5**, 235–248.

50 F. Pereira and J. Aires-de-Sousa, *J. Cheminf.*, 2018, **10**, 43.

51 *Gaussian 16, Revision C.01*, ed. M. J. Frisch, G. W. Trucks, H. B. Schlegel, G. E. Scuseria, M. A. Robb, J. R. Cheeseman, G. Scalmani, V. Barone, G. A. Petersson, H. Nakatsuji, X. Li, M. Caricato, A. V. Marenich, J. Bloino, B. G. Janesko, R. Gomperts, B. Mennucci, H. P. Hratchian, J. V. Ortiz, A. F. Izmaylov, J. L. Sonnenberg, D. Williams-Young, F. Ding, F. Lipparini, F. Egidi, J. Goings, B. Peng, A. Petrone, T. Henderson, D. Ranasinghe, V. G. Zakrzewski, J. Gao, N. Rega, G. Zheng, W. Liang, M. Hada, M. Ehara, K. Toyota, R. Fukuda, J. Hasegawa, M. Ishida, T. Nakajima, Y. Honda, O. Kitao, H. Nakai, T. Vreven, K. Throssell, J. A. Montgomery, Jr., J. E. Peralta, F. Ogliaro, M. J. Bearpark, J. J. Heyd, E. N. Brothers, K. N. Kudin, V. N. Staroverov, T. A. Keith, R. Kobayashi, J. Normand, K. Raghavachari, A. P. Rendell, J. C. Burant, S. S. Iyengar, J. Tomasi, M. Cossi, J. M. Millam, M. Klene, C. Adamo, R. Cammi, J. W. Ochterski, R. L. Martin, K. Morokuma, O. Farkas, J. B. Foresman and D. J. Fox, Gaussian, Inc., Wallingford CT, 2016.

52 G. Kigen and G. Edwards, *BMC Pharmacol. Toxicol.*, 2017, **18**, 20.

53 I. Hubatsch, E. G. E. Ragnarsson and P. Artursson, *Nat. Protoc.*, 2007, **2**, 2111–2119.

54 K. Raniga, A. Nasir, N. T. N. Vo, R. Vaidyanathan, S. Dickerson, S. Hilcove, D. Mosqueira, G. R. Mirams, P. Clements, R. Hicks, A. Pointon, W. Stebbeds, J. Francis and C. Denning, *Cell Stem Cell*, 2024, **31**, 292–311.

55 J. Tamargo, R. Caballero, R. Gómez, C. Valenzuela and E. Delpón, *Cardiovasc. Res.*, 2004, **62**, 9–33.

56 M. C. Sanguinetti and N. K. Jurkiewicz, *J. Gen. Physiol.*, 1990, **96**, 195–215.

